SI Materials and Methods

Neuronal Differentiation

Human ESCs, and iPSCs were differentiated into neuroectodermal cells in EBs using bFGF [1]. Cells were detached from plates by 1mg/ml of dispase treatment. After 30 min incubation, intact cell colonies were harvested by centrifugation, resuspended in hES medium, and then plated on ultralow cell-attachment plates (BD Biosciences) for four days with a daily medium change. Then the medium was switched to neural induction medium (DMEM/F12 supplemented with N2, MEM NEAA solution, 2 mg/ml of heparin, and 20 ng/ml of bFGF) for two days. Next, EBs were plated in laminin-coated plates, and fed with neural induction medium every other day. To continue neuronal maturation, rosette cells were incubated with neural differentiation medium (Neurocult NS-A differentiation medium, Stem Cell Technology). hESCs and iPSCs were also differentiated into neuronal lineage by blocking BMP pathway [2] and used to obtain the neural progenitor cells (NPCS). Here, cells were dissociated by dispase treatment and plated onto ultra-low attachment plates with Neural precursor medium containing B27, bFGF (20ng/ml) and recombinant noggin (500 ng/ml) for first 2 weeks and EBs were maintained with neuro-basal medium with bFGF (20ng/ml) and EGF (20ng/ml) for additional 1 week. Mature EBs were plated onto laminin coated plated and rosettes were visible after 2-5 days. Rosettes were manually collected and cultured in neural induction medium to expand the neural progenitors. For the mature neuronal differentiation, neural progenitors were cultured in Neurocult NS-A differentiation medium.

Gene Expression Analysis

RNA was isolated from cells and used to generate cDNA by Superscript II® (Invitrogen) according to the manufacturer's protocol. The expression of pluripotency markers or differentiation markers was calculated by performing real time quantitative PCR using the DyNAmo™ SYBR® Green qPCR kit (NEB). The qPCR data were analyzed by comparative threshold cycle (CT) method (delta-delta CT method) [3]. All qPCR assays were performed in triplicates with β-ACTIN as a reference and with the primers listed in Supplementary Table 2. Primers for recognizing total genes, endogenous genes, and ectopic genes used for reprogramming (OCT4, SOX2, KLF4, MYC) were listed in Supplementary table 2. In order to find the allele specific expression of MeCP2, primers that specifically bound the known mutated nucleotides of MeCP2 (Supplementary Table 3) were used to amplify specific regions of MeCP2, and sequenced.

Immunostaining

iPSCs were fixed with 4% paraformaldehyde and immunostained for pluripotency markers using the antibodies listed in Supplementary Table 4. In order to confirm the status of X chromosomes, parental fibroblast and iPSCs were fixed, stained with OCT4 and H3K27me3 antibodies. After neuronal differentiation, cells were fixed and used to confirm the expression of neuronal markers using antibodies listed in Supplemental Table 4. For the comparison between wild type RTT-iPSCs and mutant RTT-iPSCs in Figure 3C and 3D, we have performed four independent neuronal differentiation experiments. Three cellular images were taken from the representative experiment to calculate the percentage of cells expressing NESTIN, GFAP, or TuJ. Image-J software was used to process the NESTIN, GFAP, and TuJ images and to calculate the percentage of cells expressing the markers [4].

Teratoma Formation Assay

2-3x10^6 iPSCs were collected by collagenase treatment, and resuspended in DMEM/F12, collagen, and matrigel mix (2:1:1 ratio). Cells were intramuscularly injected into immunodeficient Rag2-/-GammaC-/- mice. After 6–8 weeks, teratomas were harvested, fixed, and subjected to paraffin-embedding and haematoxylin and eosin (H/E) staining.

Karyotypes

Chromosomal analysis of iPSCs was performed by Cell Line Genetics (Madison, WI) using standard high-resolution G banding.

Determination of Apoptotic Cells

RTT-iPS cell derived NPCs were differentiated into mature neuron on Laminin /Poly-L-lysine coated plates. NPCs and 8 day differentiated neurons were treated with trypsin and accutase, and subjected to apoptosis assay using Annexin V–FITC/PI Apoptosis Detection Kit (BD Pharmingen) according to the manufacturer's protocol. Apoptotic cell death was also examined by trypan blue staining.

1. Li, X.J., and Zhang, S.C. (2006). In vitro differentiation of neural precursors from human embryonic stem cells. Methods Mol Biol *331*, 169-177.
2. Gerrard, L., Rodgers, L., and Cui, W. (2005). Differentiation of human embryonic stem cells to neural lineages in adherent culture by blocking bone morphogenetic protein signaling. Stem Cells *23*, 1234-1241.
3. Livak, K.J., and Schmittgen, T.D. (2001). Analysis of relative gene expression data using real-time quantitative PCR and the 2(-Delta Delta C(T)) Method. Methods *25*, 402-408.
4. Abramoff, M.D., Magelhaes, P.J., and Ram, S.J. (2004). Image Processing with ImageJ. Biophotonics International *11*, 36-42.

Supplementary Figure Legends

Figure S1. Expression of pluripotency markers in RTT- iPSC lines.
(*A-D*) iPSCs derived from different RTT fibroblasts showed expression of pluripotent markers (SSEA3, SSEA4, TRA-1-60, TRA-1-81, OCT4, and NANOG). Regardless of the status of X chromosome inactivation and MeCP2 expression, all RTT-iPS cells similarly expressed pluripotency markers. iPSCs monoallelically expressing wild type MeCP2: RTT1-iPS16w, RTT2-iPS-42w, RTT4-iPS-24w, RTT5-iPs-32w; iPS cells monoallelically expressing only mutant MeCP2: RTT2-iPS-12m, RTT3-iPS-46m; iPS cells biallellically expressing both wild type and mutant MeCP2: RTT4-iPS-19bi, RTT5-iPS-31bi.

Figure S2. Expression of pluripotency genes in RTT- iPSC lines.
(A-D) Quantitative real time RT-PCR analysis was performed to measure the expression levels of the pluripotency markers: OCT4, SOX2, KLF4, MYC and NANOG in iPSCs, their parental fibroblasts and H1 hESCs. Comparative CT method was used. Gene expression was normalized against *β*-actin. Gene expression in iPSCs relative to that of fibroblasts was plotted. Data shown are mean ± SEM in triplicate experiments. *(E)* Semi quantitative PCR analysis was performed to examine the expression of endogenous and retroviral genes in RTT-iPSCs. While endogenous OCT4, SOX2, KLF4 and MYC are reactivated in RTT-iPSCs, ectopic genes are silenced, confirming the faithful reprogramming.

Figure S3. RTT fibroblast-derived iPSCs have a normal karyotype.
(*A-D*) G-banding analysis showed normal karyotypes of RTT-derived iPSC lines.

Figure S4. RTT-iPSCs are pluripotent.
(*A-H*) iPSCs were intramuscularly injected into immune-deficient Rag2-/-GammaC-/- mice and teratomas were harvested from 6–8 weeks, and used for Hematoxylin and Eosin (H/E) staining. Teratomas from RTT-iPSCs contained tissues of all three germ layers, confirming their *in vivo* pluripotency (endoderm tissue: intestinal endothelium or respiratory epithelium; mesoderm tissue: smooth muscles, cartilage or bone; and ectoderm tissue: pigmented epithelium or neural rosettes).

Figure S5. Allele specific MeCP2 expression in RTT-iPSC lines.

(*A*-*C*) MeCP2 was amplified from total RNA in the RTT-iPSCs, and subjected to sequencing using primers listed in supplementary table 2. RTT-iPSC clones expressed either a wild type or mutant allele of MeCP2 (RTT2-iPS-12w, RTT2-iPS-13m, RTT3-iPS-42w, RTT3-iPS-46m and RTT5-iPS-31w), or both alleles (RTT5-iPS-32bi).

Figure S6. X chromosome inactivation status in RTT-iPSCs.

RTT-iPSCs and their parental fibroblasts were stained with OCT4 antibody, H3K27me3 antibody, and DAPI (*A*-*C*). Some iPSC lines (RTT2-iPS-16w, RTT2-iPS-12m, RTT3-iPS-42w, RTT3-iPS-46m, RTT5-iPS-31w) retained the inactive X chromosome of the parental fibroblasts, while other line (RTT5-iPS-32bi) regained the activity of both X chromosomes.

Figure S7. X chromosome inactivation status in hESCs and normal iPSCs.

hESC lines and normal iPSC lines were stained for OCT4 and H3K27me3. (*A*) Male (H1) and biallelic female (H9) ES cells do not have H3K27me3 foci. (*B*-*C*) H3K27me3 staining for normal iPSCs derived from female fetal lung fibroblast (Detroit 551) and adult skin fibroblasts (PGP9f). Reprogramming of normal fibroblasts without MeCP2 mutations also show the generation of iPSC lines that either retain the inactive X chromosome or reactivate the inactive X chromosome.

Figure S8. X chromosome inactivation status in under cellular stress.

(*A*) Representative image of H3K27me3 of RTT-iPSCs after long-term culture. (*B*) Representative image of H3K27me3 staining in iPSCs expanded after freezing and thawing. Even after exposed to stress conditions, RTT-iPSCs maintain the same X chromosome inactivation status as before exposed.

Figure S9. Neuronal differentiation from RTT-iPSC lines.

(*A*) Expression of NESTIN in RTT3-iPSCs undergoing a neural differentiation protocol for 11 days. (*B*-*C*) Immunostaining of GFAP and TuJ in RTT3-iPSCs undergoing a neural differentiation protocol for 25 days.

(*D*) Expression of NESTIN in RTT4-iPSCs undergoing a neural differentiation protocol for 11 days. (*E*-*F*) Immunostaining of GFAP and TuJ in RTT4-iPSCs undergoing a neural differentiation protocol for 25 days.

While the neuronal cells differentiated from mutant RTT-iPSCs do no show difference in NESTIN and GFAP expression, they show less TuJ expression than those from H1 hESCs and wild type monoallelic RTT-iPSCs.

Figure S10. Neuronal differentiation from hESCs and iPSCs.
(*A-B*) hESCs (EOS2-DL3), normal iPSCs (PGP1-iPS1), and RTT-iPSCs (RTT5-iPS-13w and RTT5-iPS-32bi) were stained with TuJ and GFAP 25 days after differentiation. Biallelic RTT5-iPS-32bi cells showed less TuJ staining than other cells. All cell lines showed similar GFAP expression.

Figure S11. Neuronal differentiation from RTT-iPSC-derived homogenous NPCS.
(*A*) Immunostaining for NESTIN in NPCs derived hESCs (H1), normal iPSCs (551-iPS-K1, PGP9f-iPS-1), and RTT-iPSCs (RTT4-iPS-24w and RTT4-iPS19bi). All iPSC-derived NPCs are positive for NESTIN. (*B*) Immunostaining for TuJ in neuron derived from NPCs. While there was no difference in expression of NESTIN, neurons from NPCs derived from biallelic RTT4-iPS-19bi showed less TuJ expression compared with hESCs, normal iPSCs and wild type RTT4-iPS-24w cells.

Figure S12. Expression of neuronal markers during iPSC differentiation.
(*A-D*) Expression of neuronal markers during neural differentiation was analyzed by quantitative real time PCR. qPCR was performed in triplicates, and the average is represented with standard error. Change in gene expression relative to that at Day 0 is represented in logarithmic scale. While wild type RTT4-iPS-24w cells showed induction of mature neuronal marker (TuJ) at a similar level as hES cells, mutant RTT4-iPS-19bi showed less induction. hESCs and wild type or mutant biallelic iPSCs showed the similar expression of glial marker (GFAP).

Figure S13. Quantification of RTT-iPS cells undergoing apoptosis.
RTT-iPS-derived NPCs (*AB*) and mature neurons (*DE*) were examined by Annexin V/PI FACS assay. FACS assay revealed the early apoptotic cells (bottom right quadrant), vial cells (bottom left quadrant) and necrotic cells (top right quadrant). There was no difference in apoptotic or necrotic cells in NPCs or neurons from wild type and mutant RTT-iPS cells. (*CF*) The apoptotic cell death of NPCs (C) and mature neurons (F) was measured by trypan blue staining. Consistent with the result from AnnexinV/PI FACS, difference in apoptosis was not observed between wild type and mutant RTT-iPS cells. Data are mean±SD of three independent experiments.

Table S1. iPS cell clones isolated and analyzed.

Experiments/Clones	RTT1-iPSC GM17880			RTT2-iPSC GM16548			RTT3-iPSC GM07982			RTT4-iPSC GM11270			RTT5-iPSC GM17567			551-iPSC		PGP9f-iPSC	
Derived	12			8			10			11			9			7		5	
Allele Specificity of MeCP2	W	M	Bi	W	M	Bi	W	M	Bi	W	M	Bi	W	M	Bi	Mono	Bi	Mono	Bi
	3	3	4	2	3	2	3	2	3	3	4	4	2	2	3	5	2	3	2
H3K27me3	6			6			6			5			5			7		5	
Karyotype	2			2			2			2			2			N/A		1	
Teratoma	2			2			2			2			2			N/A		2	
EZH2	4			4			5			5			3			N/A		N/A	
Neural differentiation	2			N/A			2			2			2			2		1	

Table S2. Primers used for real time-quantitative PCR

Gene	Forward primer	Reverse primer
ACTB	TGAAGTGTGACGTGGACATC	GGAGGAGCAATGATCTTGAT
NANOG	TGAACCTCAGCTACAAACAG	TGGTGGTAGGAAGAGTAAAG
Total OCT4	AGCGAACCAGTATCGAGAAC	TTACAGAACCACACTCGGAC
Total SOX2	AGCTACAGCATGATGCAGGA	GGTCATGGAGTTGTACTGCA
Total KLF4	TCTCAAGGCACACCTGCGAA	TAGTGCCTGGTCAGTTCATC
Total cMYC	ACTCTGAGGAGGAACAAGAA	TGGAGACGTGGCACCTCTT
Endo-OCT4	CCTCACTTCACTGCACTGTA	CAGGTTTTCTTTCCCTAGCT
Endo-SOX2	CCCAGCAGACTTCACATGT	CCTCCCATTTCCCTCGTTTT
Endo-KLF4	GATGAACTGACCAGGCACTA	GTGGGTCATATCCACTGTCT
Endo-cMYC	TGCCTCAAATTGGACTTTGG	GATTGAAATTCTGTGTAACTGC
Ecto-OCT4	CCTCACTTCACTGCACTGTA	CCTTGAGGTACCAGAGATCT
Ecto-SOX2	CCCAGCAGACTTCACATGT	CCTTGAGGTACCAGAGATCT
Ecto-KLF4	GATGAACTGACCAGGCACTA	CCTTGAGGTACCAGAGATCT
Ecto-cMYC	TGCCTCAAATTGGACTTTGG	CGCTCGAGGTTAACGAATT
PAX6	TGGGCGCAGACGGCATGTAT	CGTAGGTTGCCCTGGCACCG
SCNA	ATCGGCAATTCCGTGGGGGC	CCCACACAGCACGCGGAACA
SCNB	ATCTCCTGCAAGCGCCGCAG	GTGGCACTCGTAGTCGCCCG
GFAP	TGCTCGCCGCTCCTACGTCT	ATCCACCCGGGTCGGGAGTG
SOX1	GATCAGCAAGCGCCTGGGGG	AGCAGCGTCTTGGTCTTGCGG
TuJ	GCCGCTACCTGACGGTGGC	GGGCGGGATGTCACACACGG
BDNF	CCACCAGGTGAGAAGAGTGATGACCA	GCCTTGGGCCCATTCACGCT
MECP2	AGAAACGGGGCCGAAAGCCG	GCAACCGCGGGCTGAGTCTT
EZH2	ACCGGTTGTGGGCTGCACAC	TGCAGCGGCATCCCGGAAAG

Table S3. Sequences of primers used to amplify and sequence MeCP2.

Cell Line	Forward & sequencing primer	Reverse primer
RTT1	ATGGCCGCCGCTGCCGCCACCGCC	CACCACTTCCTTGACCTCGA
RTT2 RTT3 RTT4	AGGTAGGCGACACATCCCT	CTTACAGGTCTTCAGGACCTT
RTT5	AGAAACGGGGCCGAAAGCCG	CGGGAAGCTTTGTCAGAGCC

Table S4. Antibodies used in this study

Antibody	Catalogue Number	Company
OCT4	Ab19857	Abcam
Tra-1-60	BD560173	BD Biosciences
Tra-1-81	BD560174	BD Biosciences
SSEA3	MAB4303	Milipore
SSEA4	BD560218	BD Biosciences
NANOG	Ab21624	Abcam
TuJ	Sc-58888	Santa Cruz
TuJ	ab18207	Abcam
GFAP	MO15052	Gentaur
NESTIN	Sc-71665	Santa Cruz
H3K27me3	Rabbit mAb #9733	Cell signaling technology
Alexa Fluor 488	A11001, A11008	Invitrogen
Alexa Fluor 555	A31572, A21422	Invitrogen

Figure S1.

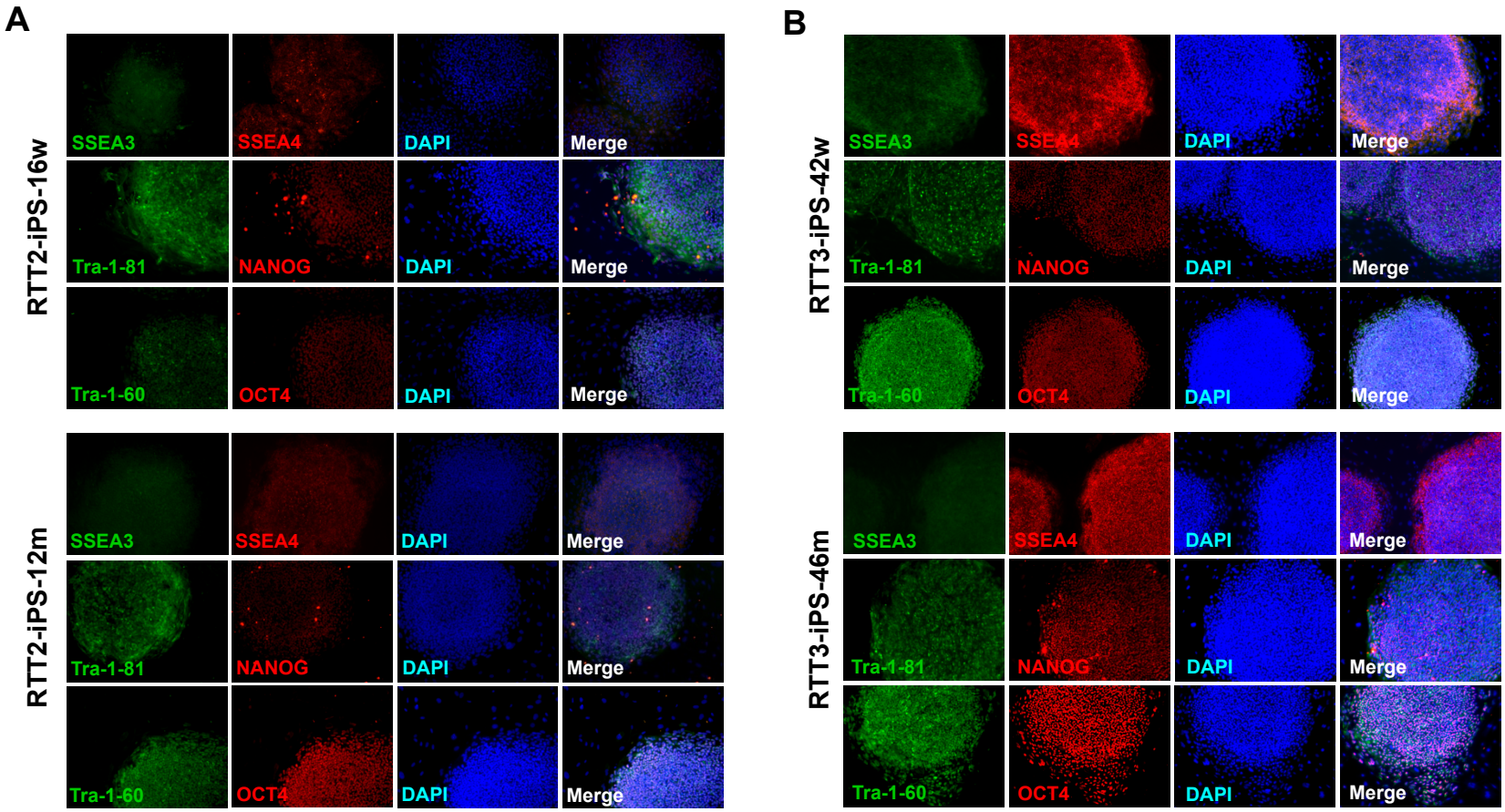
A
RTT2-iPS-16w
SSEA3
SSEA4
DAPI
Merge
Tra-1-81
NANOG
DAPI
Merge
Tra-1-60
OCT4
DAPI
Merge
RTT2-iPS-12m
SSEA3
SSEA4
DAPI
Merge
Tra-1-81
NANOG
DAPI
Merge
Tra-1-60
OCT4
DAPI
Merge
B
RTT3-iPS-42w
SSEA3
SSEA4
DAPI
Merge
Tra-1-81
NANOG
DAPI
Merge
Tra-1-60
OCT4
DAPI
Merge
RTT3-iPS-46m
SSEA3
SSEA4
DAPI
Merge
Tra-1-81
NANOG
DAPI
Merge
Tra-1-60
OCT4
DAPI
Merge

Figure S1.

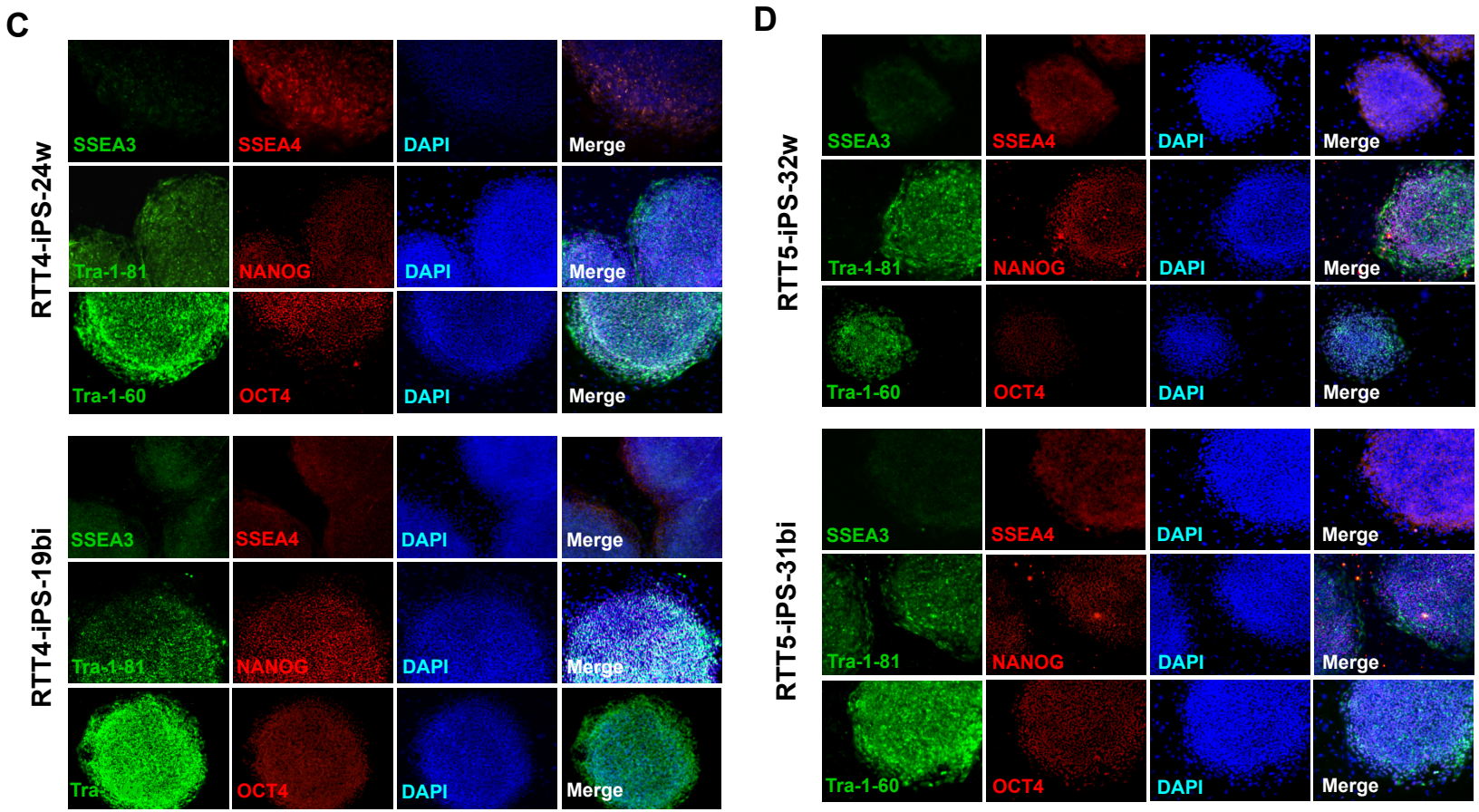
C
RTT4-iPS-24w
SSEA3
SSEA4
DAPI
Merge
Tra-1-81
NANOG
DAPI
Merge
Tra-1-60
OCT4
DAPI
Merge
RTT4-iPS-19bi
SSEA3
SSEA4
DAPI
Merge
Tra-1-81
NANOG
DAPI
Merge
Tra-
OCT4
DAPI
Merge
D
RTT5-iPS-32w
SSEA3
SSEA4
DAPI
Merge
Tra-1-81
NANOG
DAPI
Merge
Tra-1-60
OCT4
DAPI
Merge
RTT5-iPS-31bi
SSEA3
SSEA4
DAPI
Merge
Tra-1-81
NANOG
DAPI
Merge
Tra-1-60
OCT4
DAPI
Merge

Figure S2.

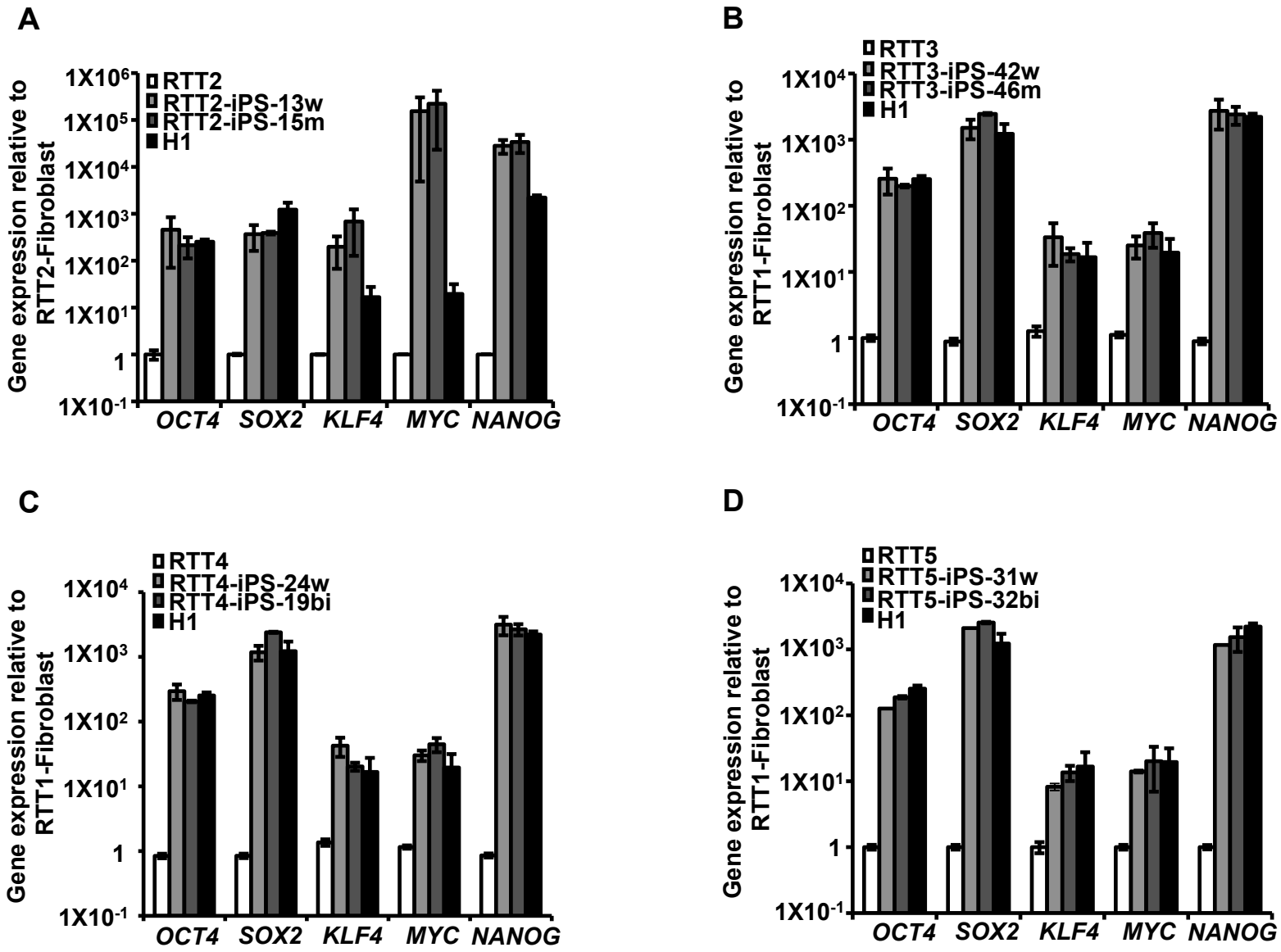
A
Gene expression relative to RTT2-Fibroblast
RTT2
RTT2-iPS-13w
RTT2-iPS-15m
H1
1X10^6
1X10^5
1X10^4
1X10^3
1X10^2
1X10^1
1
1X10^-1
OCT4
SOX2
KLF4
MYC
NANOG
B
Gene expression relative to RTT1-Fibroblast
RTT3
RTT3-iPS-42w
RTT3-iPS-46m
H1
1X10^4
1X10^3
1X10^2
1X10^1
1
1X10^-1
OCT4
SOX2
KLF4
MYC
NANOG
C
Gene expression relative to RTT1-Fibroblast
RTT4
RTT4-iPS-24w
RTT4-iPS-19bi
H1
1X10^4
1X10^3
1X10^2
1X10^1
1
1X10^-1
OCT4
SOX2
KLF4
MYC
NANOG
D
Gene expression relative to RTT1-Fibroblast
RTT5
RTT5-iPS-31w
RTT5-iPS-32bi
H1
1X10^4
1X10^3
1X10^2
1X10^1
1
1X10^-1
OCT4
SOX2
KLF4
MYC
NANOG

Figure S2.

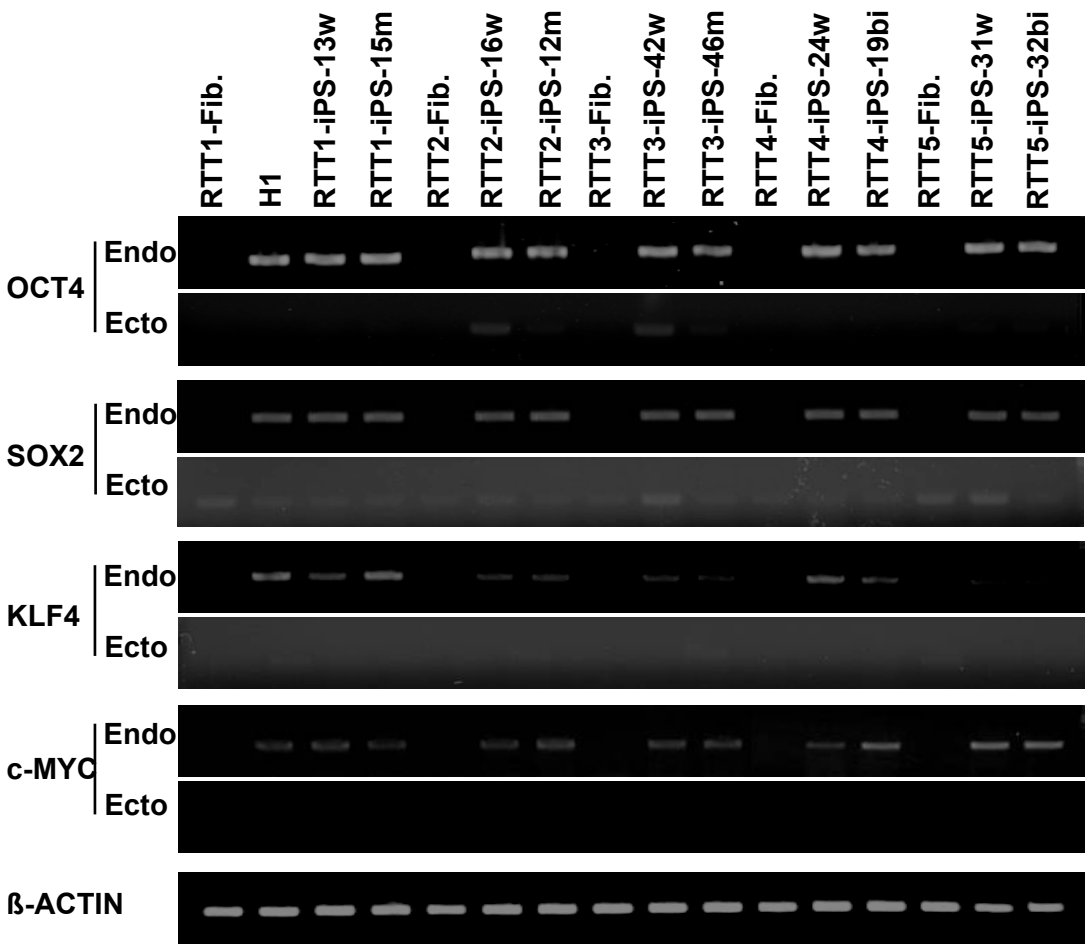
E
RTT1-Fib.
H1
RTT1-iPS-13w
RTT1-iPS-15m
RTT2-Fib.
RTT2-iPS-16w
RTT2-iPS-12m
RTT3-Fib.
RTT3-iPS-42w
RTT3-iPS-46m
RTT4-Fib.
RTT4-iPS-24w
RTT4-iPS-19bi
RTT5-Fib.
RTT5-iPS-31w
RTT5-iPS-32bi
OCT4
Endo
Ecto
SOX2
Endo
Ecto
KLF4
Endo
Ecto
c-MYC
Endo
Ecto
ß-ACTIN

Figure S3.

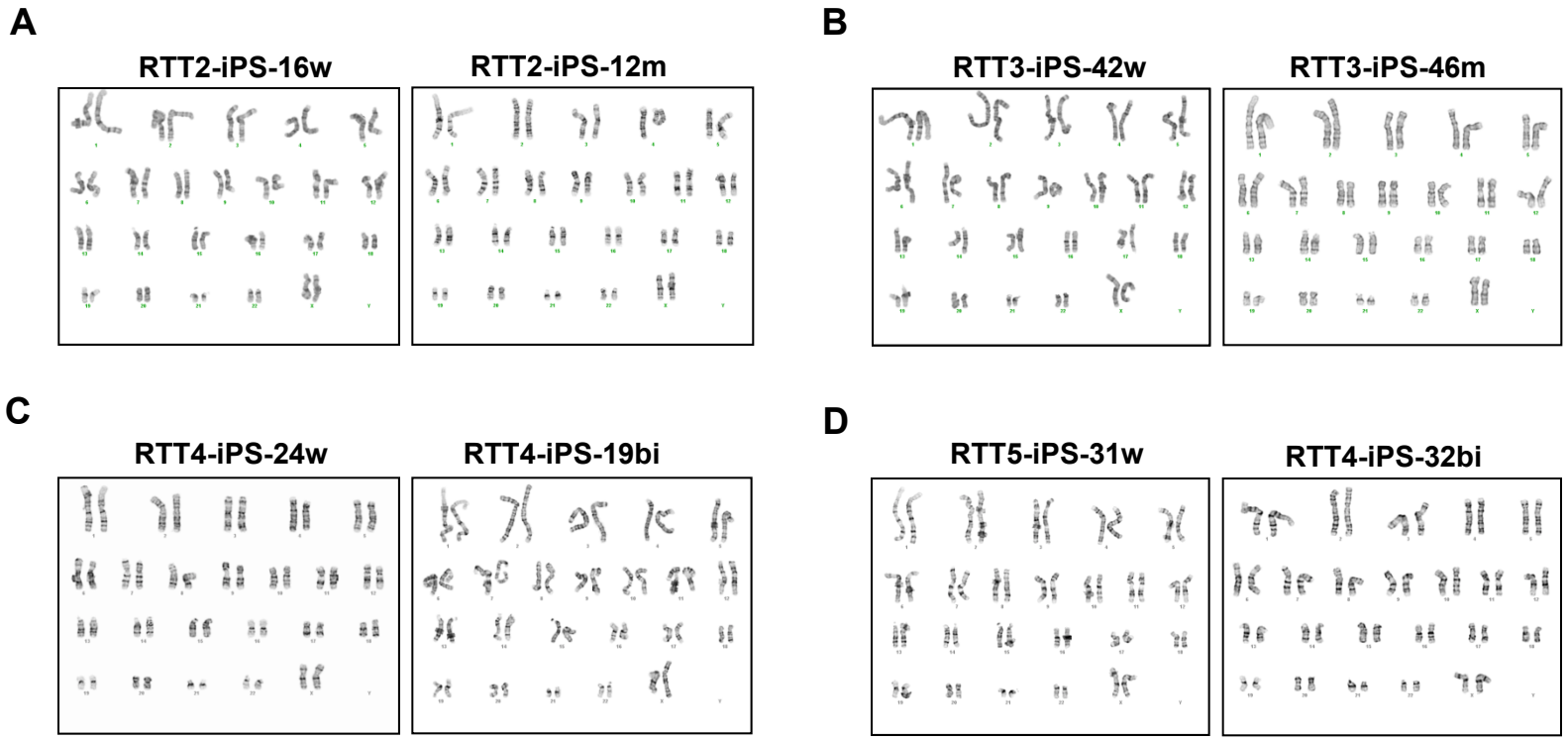
A
RTT2-iPS-16w
RTT2-iPS-12m
B
RTT3-iPS-42w
RTT3-iPS-46m
C
RTT4-iPS-24w
RTT4-iPS-19bi
D
RTT5-iPS-31w
RTT4-iPS-32bi

Figure S4.

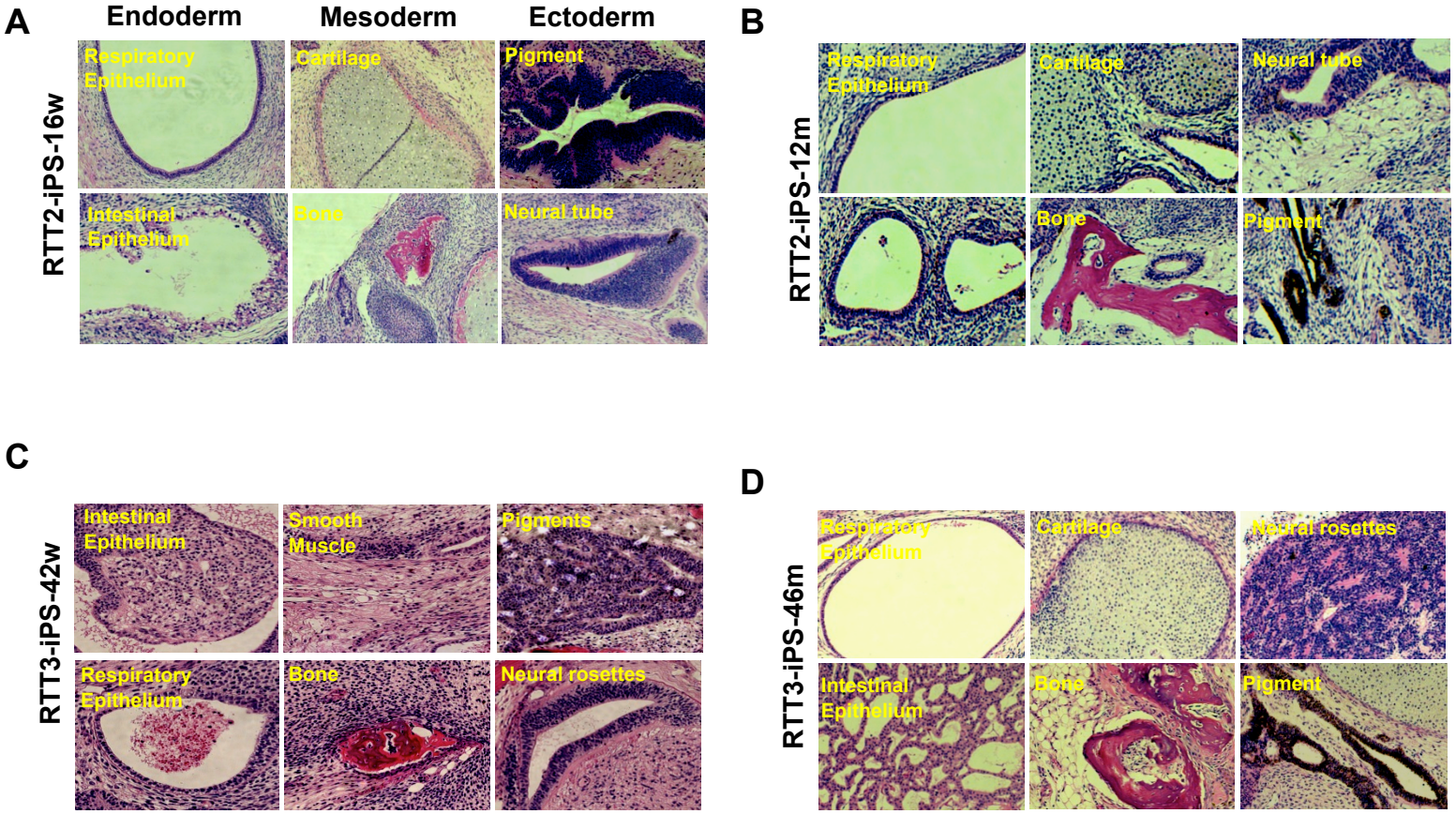
A
Endoderm
Mesoderm
Ectoderm
RTT2-iPS-16w
Respiratory Epithelium
Cartilage
Pigment
Intestinal Epithelium
Bone
Neural tube
B
RTT2-iPS-12m
Respiratory Epithelium
Cartilage
Neural tube
Bone
Pigment
C
RTT3-iPS-42w
Intestinal Epithelium
Smooth Muscle
Pigments
Respiratory Epithelium
Bone
Neural rosettes
D
RTT3-iPS-46m
Respiratory Epithelium
Cartilage
Neural rosettes
Intestinal Epithelium
Bone
Pigment

Figure S4.

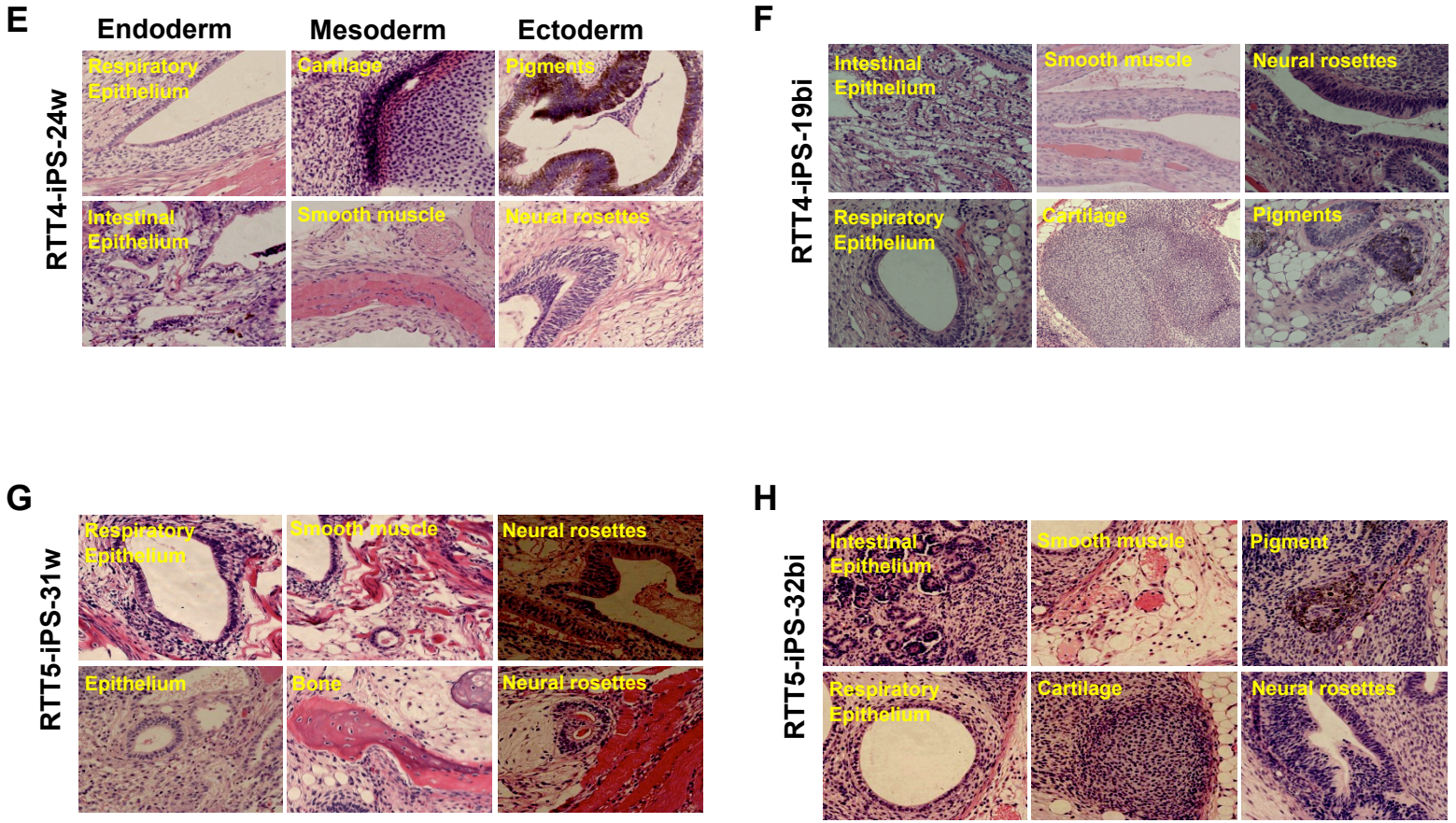
E
Endoderm
Mesoderm
Ectoderm
RTT4-iPS-24w
Respiratory Epithelium
Cartilage
Pigments
Intestinal Epithelium
Smooth muscle
Neural rosettes
F
RTT4-iPS-19bi
Intestinal Epithelium
Smooth muscle
Neural rosettes
Respiratory Epithelium
Cartilage
Pigments
G
RTT5-iPS-31w
Respiratory Epithelium
Smooth muscle
Neural rosettes
Epithelium
Bone
Neural rosettes
H
RTT5-iPS-32bi
Intestinal Epithelium
Smooth muscle
Pigment
Respiratory Epithelium
Cartilage
Neural rosettes

Figure S5.

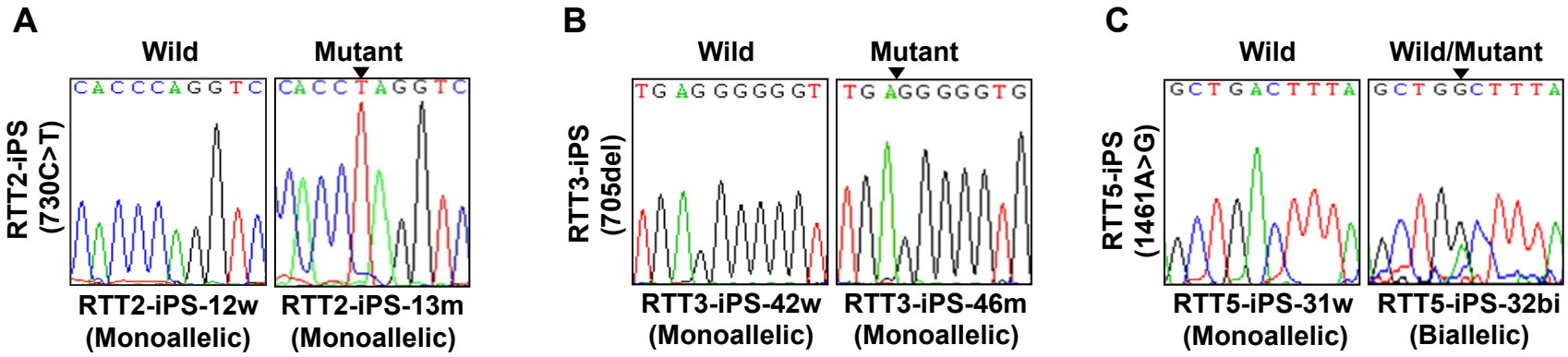
A
Wild
Mutant
RTT2-iPS (730C>T)
RTT2-iPS-12w (Monoallelic)
RTT2-iPS-13m (Monoallelic)
B
Wild
Mutant
RTT3-iPS (705del)
RTT3-iPS-42w (Monoallelic)
RTT3-iPS-46m (Monoallelic)
C
Wild
Wild/Mutant
RTT5-iPS (1461A>G)
RTT5-iPS-31w (Monoallelic)
RTT5-iPS-32bi (Biallelic)

Figure S6.

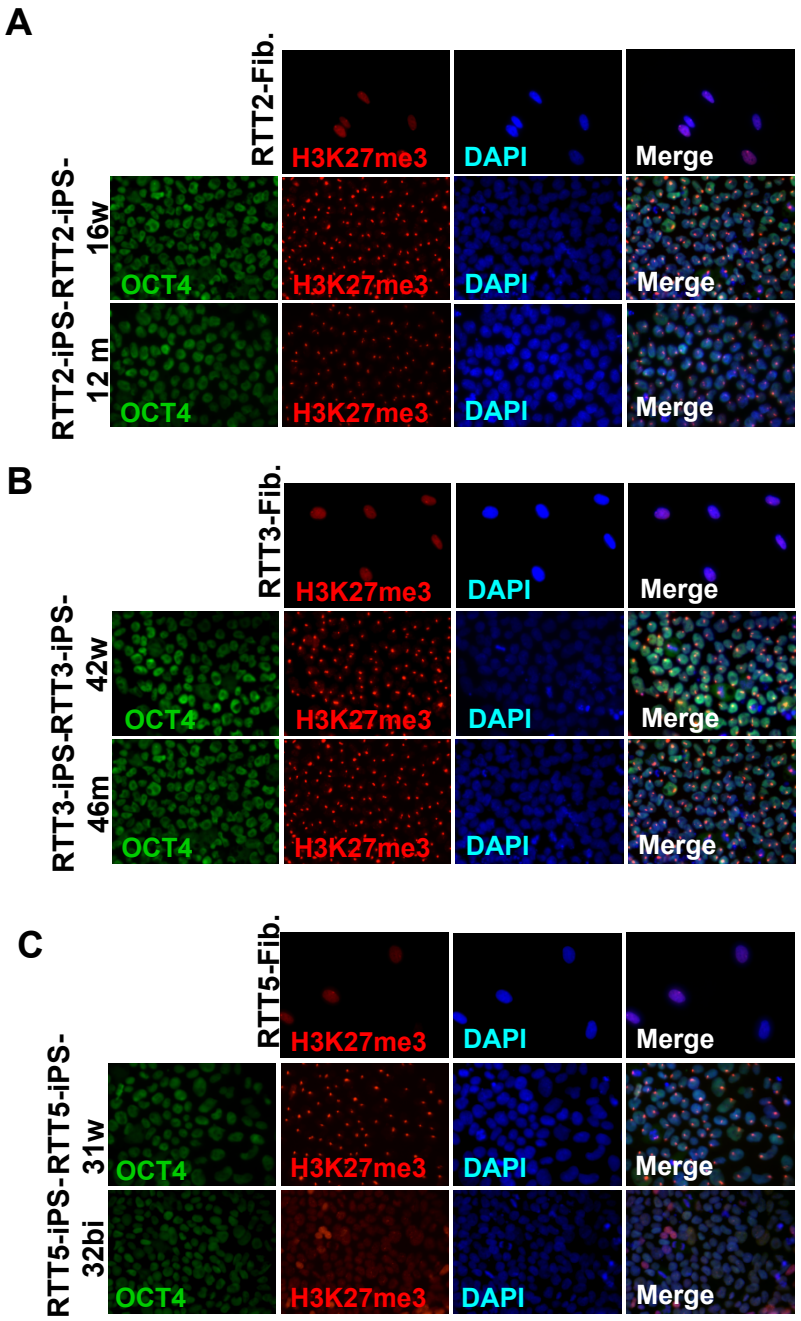
A
RTT2-Fib.
H3K27me3
DAPI
Merge
RTT2-iPS-16w
OCT4
H3K27me3
DAPI
Merge
RTT2-iPS-12 m
OCT4
H3K27me3
DAPI
Merge
B
RTT3-Fib.
H3K27me3
DAPI
Merge
RTT3-iPS-42w
OCT4
H3K27me3
DAPI
Merge
RTT3-iPS-46m
OCT4
H3K27me3
DAPI
Merge
C
RTT5-Fib.
H3K27me3
DAPI
Merge
RTT5-iPS-31w
OCT4
H3K27me3
DAPI
Merge
RTT5-iPS-32bi
OCT4
H3K27me3
DAPI
Merge

Figure S7.

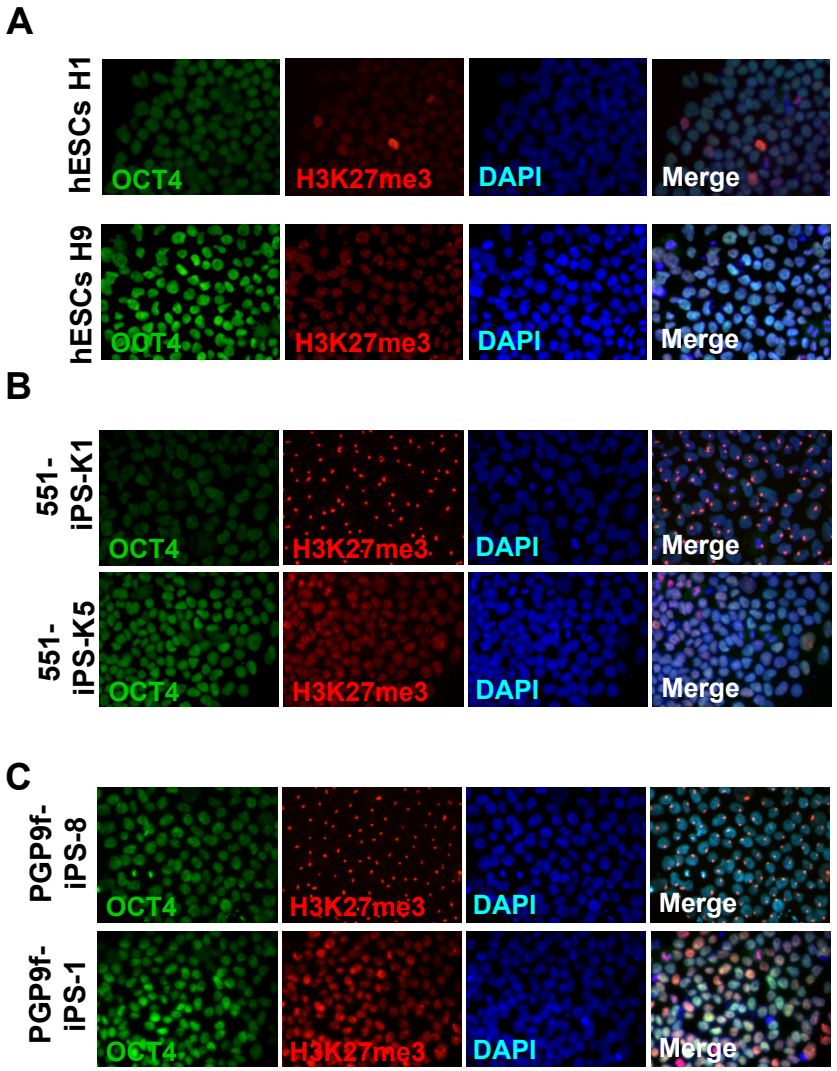
A
hESCs H1
OCT4
H3K27me3
DAPI
Merge
hESCs H9
OCT4
H3K27me3
DAPI
Merge
B
551-iPS-K1
OCT4
H3K27me3
DAPI
Merge
551-iPS-K5
OCT4
H3K27me3
DAPI
Merge
C
PGP9f-iPS-8
OCT4
H3K27me3
DAPI
Merge
PGP9f-iPS-1
OCT4
H3K27me3
DAPI
Merge

Figure S8.

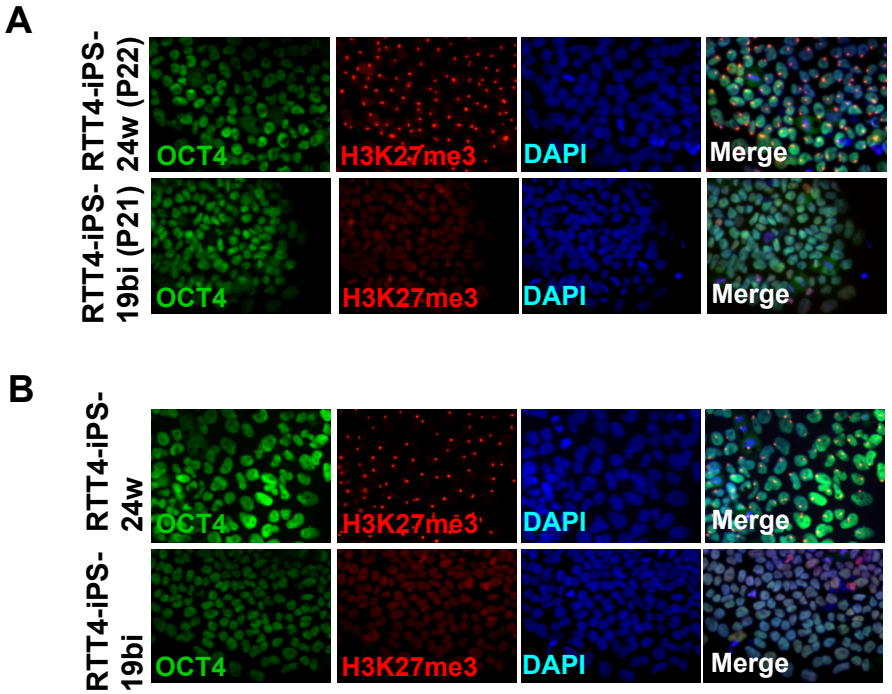
A
RTT4-iPS-24w (P22)
RTT4-iPS-19bi (P21)
OCT4
H3K27me3
DAPI
Merge
OCT4
H3K27me3
DAPI
Merge
B
RTT4-iPS-24w
RTT4-iPS-19bi
OCT4
H3K27me3
DAPI
Merge
OCT4
H3K27me3
DAPI
Merge

Figure S9.

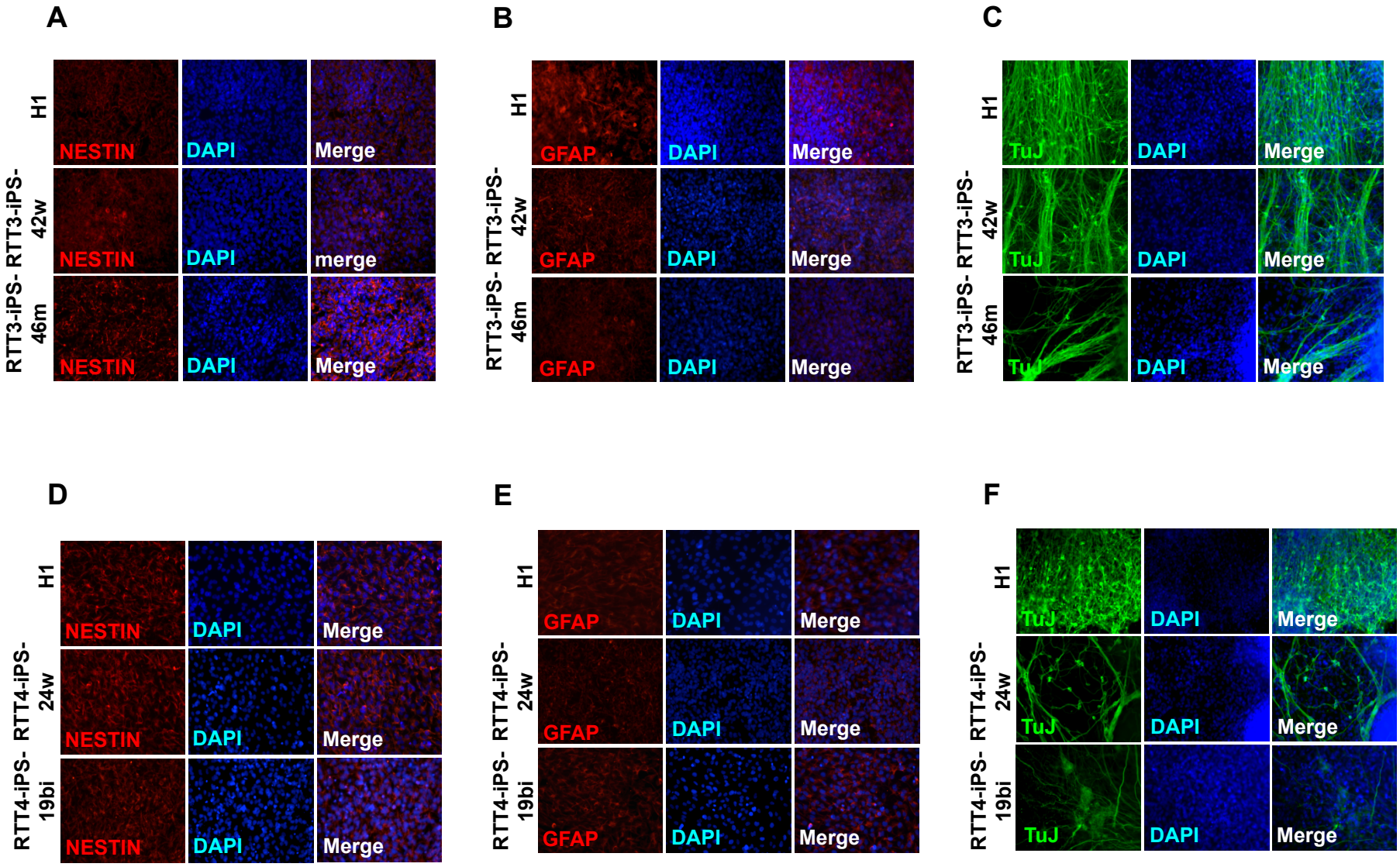
A
H1
RTT3-iPS- 42w
RTT3-iPS- 46m
NESTIN
DAPI
Merge
merge
B
GFAP
C
TuJ
D
RTT4-iPS- 24w
RTT4-iPS- 19bi
E
F

Figure S10.

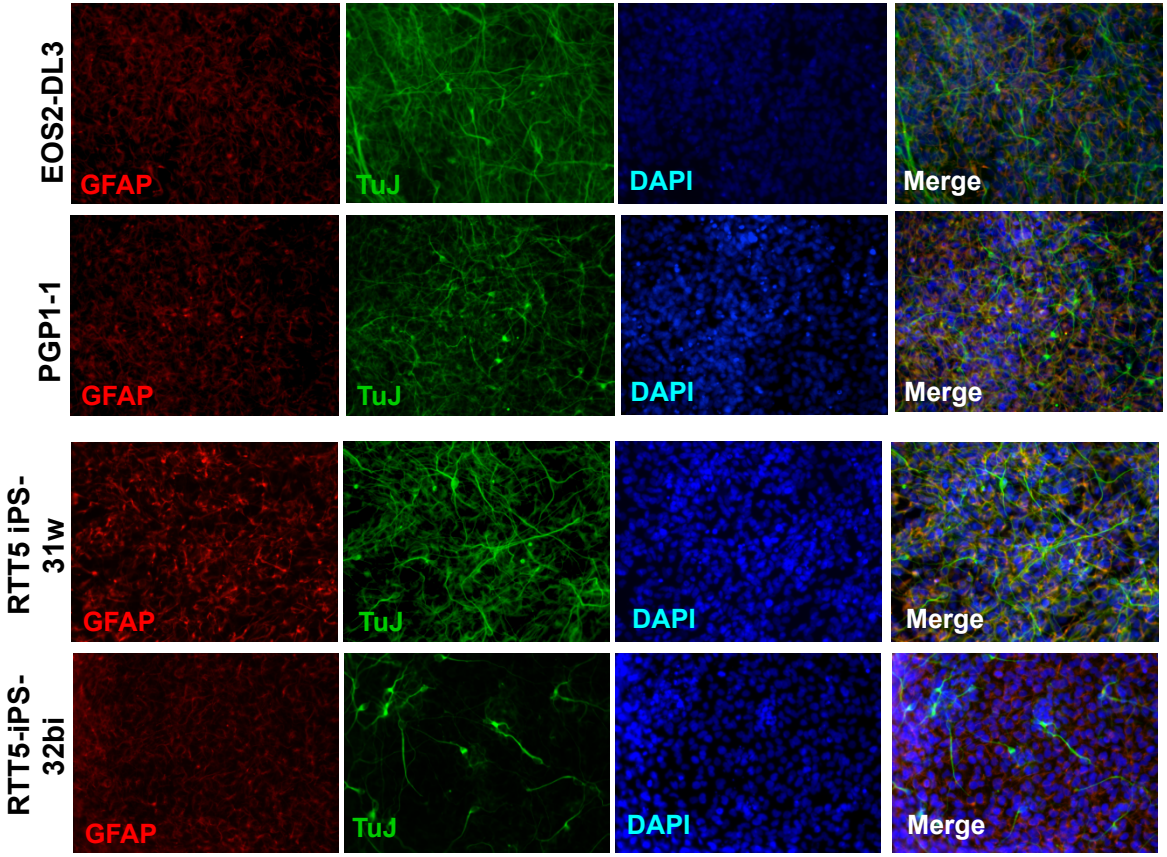

Figure S11

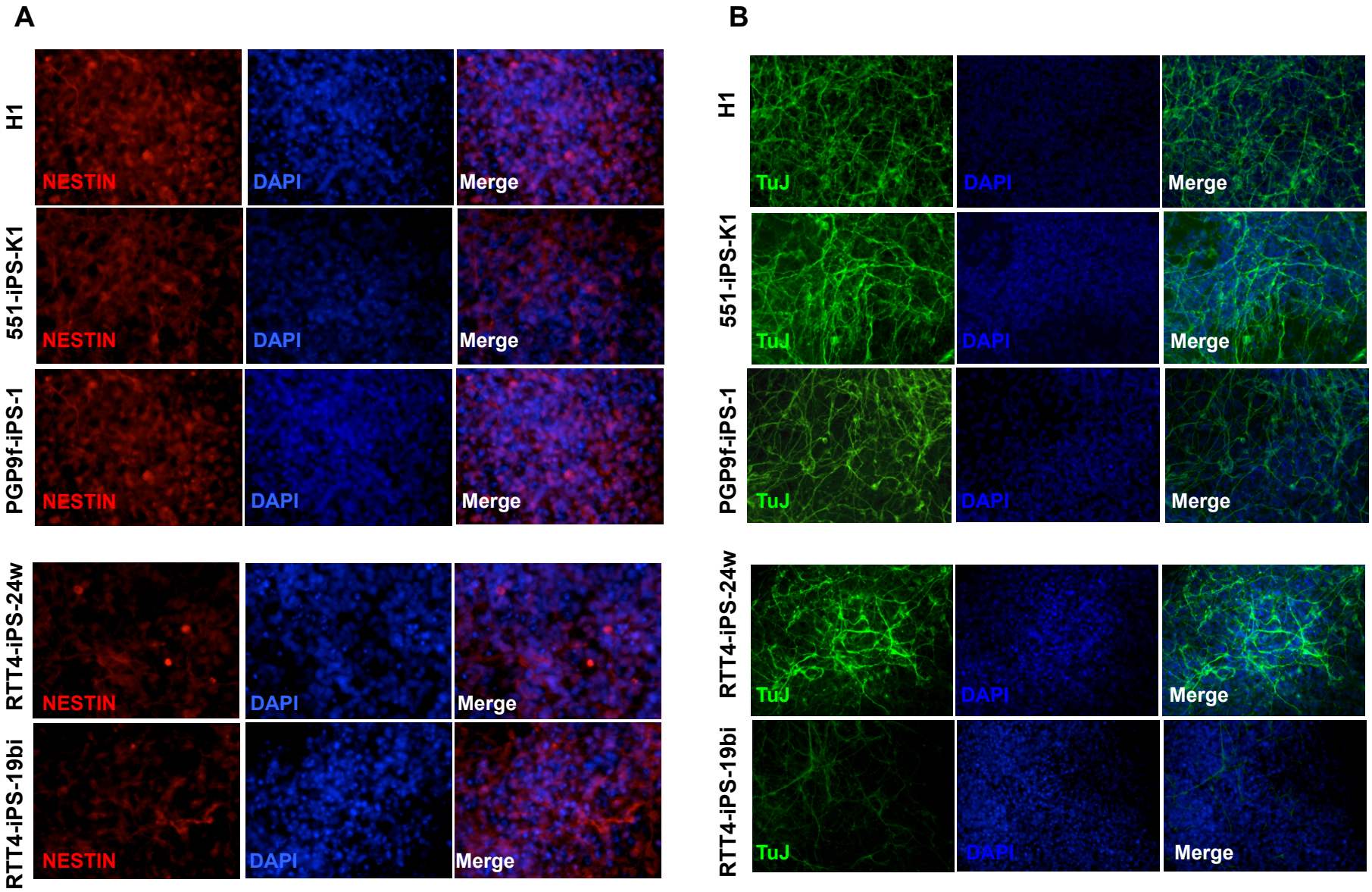
A
H1
NESTIN
DAPI
Merge
551-iPS-K1
NESTIN
DAPI
Merge
PGP9f-iPS-1
NESTIN
DAPI
Merge
RTT4-iPS-24w
NESTIN
DAPI
Merge
RTT4-iPS-19bi
NESTIN
DAPI
Merge
B
H1
TuJ
DAPI
Merge
551-iPS-K1
TuJ
DAPI
Merge
PGP9f-iPS-1
TuJ
DAPI
Merge
RTT4-iPS-24w
TuJ
DAPI
Merge
RTT4-iPS-19bi
TuJ
DAPI
Merge

Figure S12

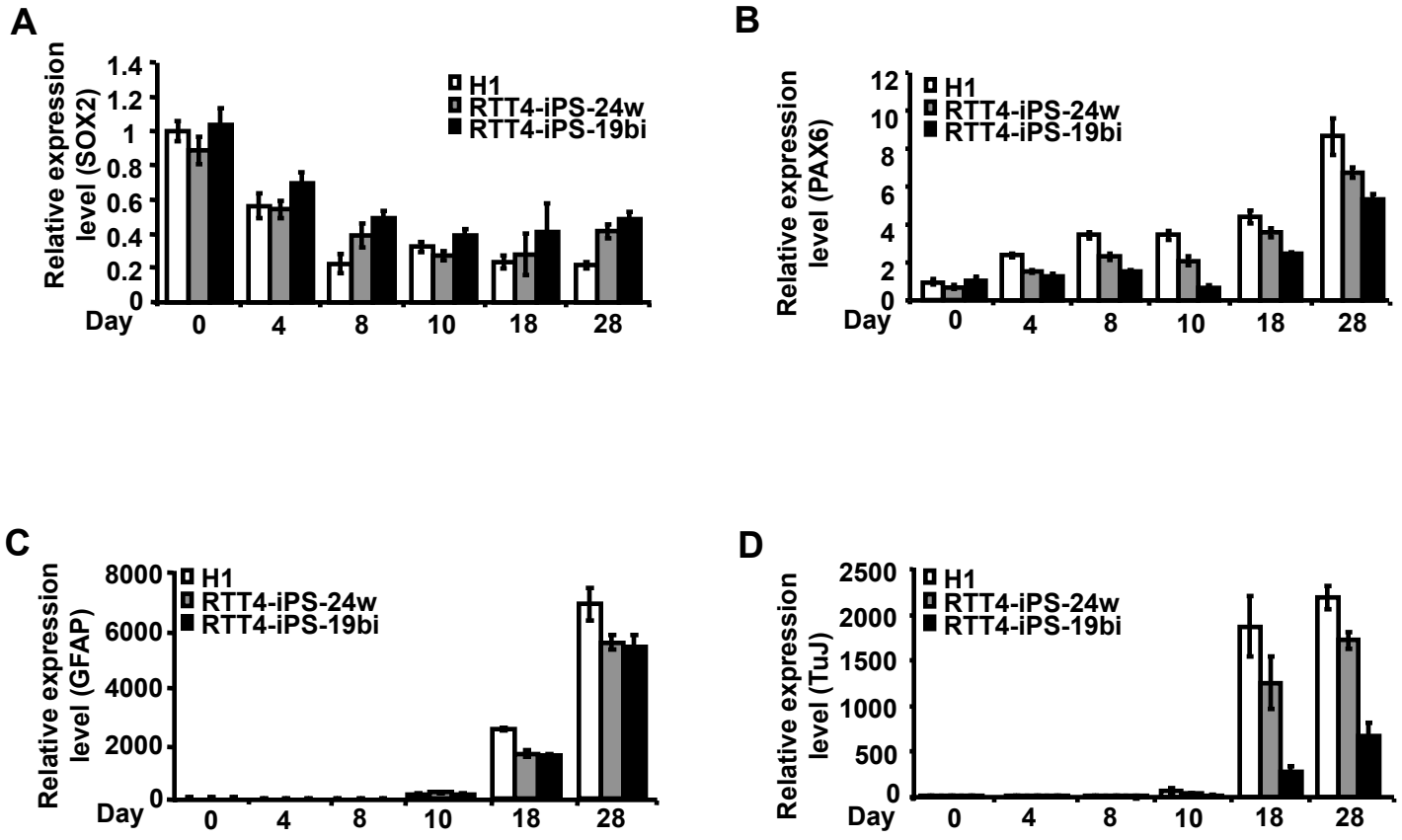
A
Relative expression level (SOX2)
1.4
1.2
1
0.8
0.6
0.4
0.2
0
Day
0
4
8
10
18
28
H1
RTT4-iPS-24w
RTT4-iPS-19bi
B
Relative expression level (PAX6)
12
10
8
6
4
2
0
C
Relative expression level (GFAP)
8000
6000
4000
2000
0
D
Relative expression level (TuJ)
2500
2000
1500
1000
500
0

Figure S13

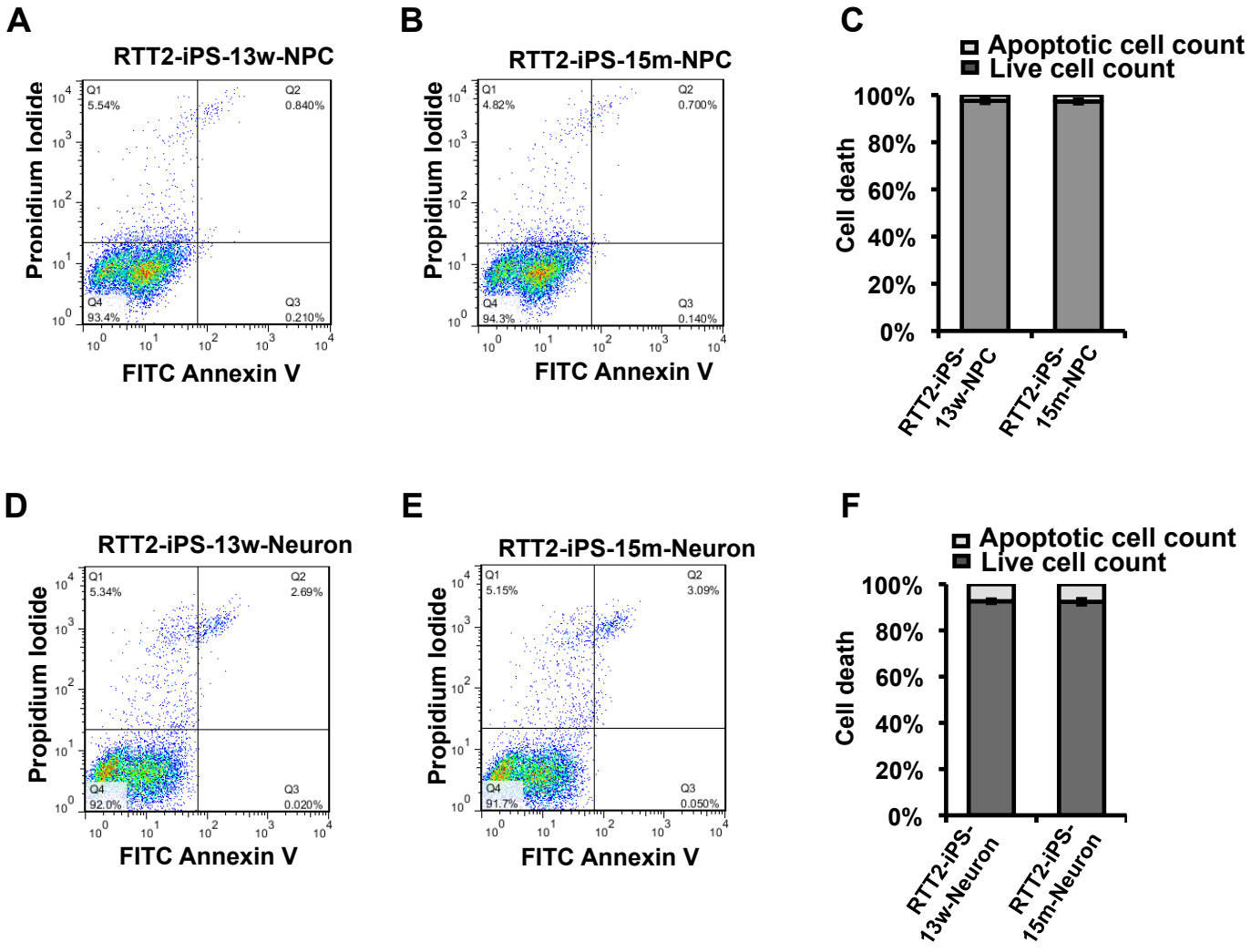
A
RTT2-iPS-13w-NPC
Propidium Iodide
FITC Annexin V
Q1 5.54%
Q2 0.840%
Q4 93.4%
Q3 0.210%
B
RTT2-iPS-15m-NPC
Q1 4.82%
Q2 0.700%
Q4 94.3%
Q3 0.140%
C
Apoptotic cell count
Live cell count
Cell death
100%
80%
60%
40%
20%
0%
RTT2-iPS-13w-NPC
RTT2-iPS-15m-NPC
D
RTT2-iPS-13w-Neuron
Q1 5.34%
Q2 2.69%
Q4 92.0%
Q3 0.020%
E
RTT2-iPS-15m-Neuron
Q1 5.15%
Q2 3.09%
Q4 91.7%
Q3 0.050%
F
Apoptotic cell count
Live cell count
Cell death
RTT2-iPS-13w-Neuron
RTT2-iPS-15m-Neuron